ELSEVIER

Materials Science and Engineering B 147 (2008) 152–155

MATERIALS SCIENCE & ENGINEERING B

www.elsevier.com/locate/mseb

Doping dependence of LO-phonon depletion scheme THz quantum-cascade lasers

Aaron Maxwell Andrews [a,*], Alexander Benz [a], Christoph Deutsch [a], Gernot Fasching [a], Karl Unterrainer [a], Pavel Klang [b], Werner Schrenk [b], Gottfried Strasser [b]

[a] *Institute for Photonics, Technical University of Vienna, Gusshausstrasse 27-29, 1040 Wien, Austria*
[b] *Center for Micro- and Nanostructures, Technical University of Vienna, Floragasse 7/392, 1040 Wien, Austria*

Received 2 July 2007; received in revised form 17 August 2007; accepted 28 August 2007

Abstract

The effect of doping on terahertz quantum-cascade lasers (QCL) utilizing the longitudinal-optical (LO)-phonon depletion scheme of the lower laser state is investigated. Five identical 2.8 THz samples were grown with 2D equivalent doping ranging from 4.3×10^9 to $3.9 \times 10^{10}\,\mathrm{cm}^{-2}$. A linear dependence on doping is observed for both the threshold current density J_{th} and maximum current density J_{max}. Only the sample doped to $3.9 \times 10^{10}\,\mathrm{cm}^{-2}$ shows the effects of free-carrier absorption with a nonlinear increase in J_{th}, while the J_{max} remained linear. Since the applied field determines when the lasing action takes place, linearity is expected when the losses are independent of doping. All samples showed a similar T_{max} of 140 K and T_0 of 30 K.
© 2007 Elsevier B.V. All rights reserved.

Keywords: Laser processing; Doping effects; Molecular beam epitaxy; Heterostructures; Superlattices; Quantum structures

1. Introduction

Since the first THz quantum-cascade laser (QCL) [1] there has been great progress in the available range of emission frequencies 1.2–4.4 THz (250–64 μm) [1–3], reduction of the threshold current to 1 A/cm^2 [4], 248 mW of peak power [3], a maximum operating temperature of 167 K [5], as well as single mode emission [6]. This has been accomplished through the understanding and improvement of the THz QCL active region and waveguide designs [7]. There are three distinct designs for the population inversion in the THz QCL active region: chirped superlattice [1], bound-to-continuum [8,9], and the LO-phonon depopulation scheme [10,11]. The first two are low threshold designs, while the third active region shows the best temperature performance [5]. The LO-phonon active region requires a high electric field for lasing (>8 kV/cm) and it is possible to reduce the threshold current by reducing the doping in the active region at the expense of emission power.

The losses in THz QCLs are often difficult to separate: free-carrier absorption, impurity scattering, interface roughness, electron–electron scattering, electron–phonon scattering, waveguide losses, and mirror losses. There have been three previous reports into the doping characteristics of THz QCL structures to study free-carrier absorption [12–14]. Liu et al. [12] studied doping in one 3.2 THz LO-phonon scheme molecular beam epitaxy (MBE) grown sample that was delta doped without rotation to provide a doping gradient within the same sample of $3.2–4.8 \times 10^{10}\,\mathrm{cm}^{-2}$ ($6.0–9.0 \times 10^{15}\,\mathrm{cm}^{-3}$ average doping density). Due to the delta doping, this study was limited to doping concentrations ±20% of the average for a 3-in. substrate and based on the maximum lasing temperature T_{max} of 109 K, $3.6 \times 10^{10}\,\mathrm{cm}^{-2}$ was determined to be the optimum dopant concentration and higher doping was believed to result in free-carrier absorption of the photons. The threshold current density J_{th} showed an increasing, but nonlinear, relationship to doping density, which is expected for free-carrier absorption.

A broader range of doping, $3.3–8.8 \times 10^{10}\,\mathrm{cm}^{-2}$ ($2.8–7.6 \times 10^{15}\,\mathrm{cm}^{-3}$ average doping density) was studied by Ajili et al. [13] in a 3.45 THz bound-to-continuum active region. A linear dependence between threshold current density J_{th} and carrier sheet density was observed, which was found to agree with the expected increased waveguide losses. Due to the active region design, changes in doping (increasing) resulted in a red shift of the THz emission frequency. This is due to the lasing

* Corresponding author. Tel.: +43 1 58801 36218; fax: +43 1 58801 36299.
E-mail address: max.andrews@tuwien.ac.at (A.M. Andrews).

0921-5107/$ – see front matter © 2007 Elsevier B.V. All rights reserved.
doi:10.1016/j.mseb.2007.08.012

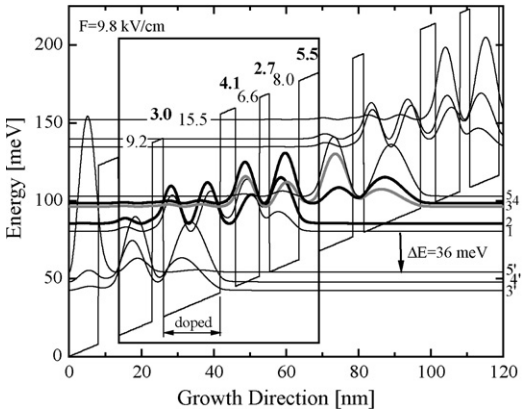

Fig. 1. Band structure and calculated squared wave functions at a field of 9.8 kV/cm for the 2.8 THz samples A–E. The GaAs well and $Al_{0.15}Ga_{0.85}As$ barrier (bold) sequence from the left is 9.2/**3.0**/15.5/**4.1**/6.6/**2.7**/8.0/**5.5** nm, where the underlined well is doped. The optical transition is between upper laser states 3 and 4 and the lower laser state 2. The lower laser state is rapidly depopulated to the next cascade, levels 5′, 4′, etc., by an LO phonon.

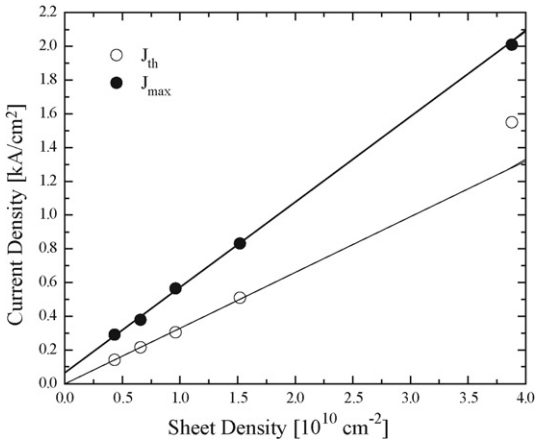

Fig. 2. Threshold current density J_{th} (open circles) and J_{max} (solid circles) as a function of carrier sheet density at 5 K. The solid lines are linear curve fits of only the first 4 lower doped samples A–D and not the highest doped sample E.

action beginning at a lower applied electric field. Unfortunately, this makes optimizing the structure for a particular frequency or wave number difficult. They did observe a strange crossover of the J_{th} and J_{max} at $3.3 \times 10^{10}\,cm^{-2}$ ($2.8 \times 10^{15}\,cm^{-3}$) and not at zero. The measured J_{max} was extrapolated to the zero current point of $2.0 \times 10^{10}\,cm^{-2}$, implying the MBE used had p-type background doping of $1.7 \times 10^{15}\,cm^{-3}$ or there was some additional problem measuring the correct doping.

In this paper, we continue to investigate doping for over an order of magnitude in the LO-phonon depopulation scheme THz QCLs to determine the influence of doping concentration on lasing performance [14].

2. Experimental

Six LO-phonon depopulation THz QCL structures designed for 2.75 THz, nearly identical to Ref. [15], were grown by solid-source MBE as described in Ref. [16]. Each sample begins with an $Al_{0.55}Ga_{0.45}As$ layer, which is used as an etch stop layer, and then a 90 nm highly doped GaAs contact layer. The subsequent cascade unit cell, shown with the calculated band structure in Fig. 1, is composed of four GaAs wells and $Al_{0.15}Ga_{0.85}As$ barriers (bold) 9.2/**3.0**/15.5/**4.1**/6.6/**2.7**/8.0/**5.5** nm thick. The doping is only in the widest well (underlined) and for the five samples A–E are, respectively, 2.80, 4.24, 6.40, 10.0, and $25.0 \times 10^{15}\,cm^{-3}$, plus an additional undoped sample (not labeled). This corresponds to a commonly used sheet density equivalent of 0.43, 0.66, 0.99, 1.55, and $3.88 \times 10^{10}\,cm^{-2}$. Doping was calibrated through the growth of Si-doped GaAs samples, which were then measured with a Hall setup. When calculating the band structure doping was neglected, but the widest well is chosen for doping so that dopant atoms coincide with the LO-phonon depopulation. To reduce waveguide losses, a 15 μm thick active region is used with 271 cascade cells. The top contact is 60 nm highly doped GaAs.

The samples were then processed into a high-confinement Au–Au double metal waveguide by thermal bonding and then the sidewalls and facets etched by reactive ion etching (RIE). The final laser cavities were 120 μm × 1000 μm. The electrical measurements were performed in pulsed mode operation with a pulse length of 100 ns at a repetition rate of 1 kHz. The short pulse length was chosen to prevent any additional heating.

3. Results and discussion

The summary of results is presented in Table 1 for samples A–E. All samples lased around 2.8 THz and deviations in emission frequency are due to growth deviations from the nominal structure. The doping range from 0.43 to $3.88 \times 10^{10}\,cm^{-2}$ is much greater than previously studied for the LO-phonon depopulation THz QCL [12,14]. The threshold current density J_{th} and J_{max} are plotted as a function of dopant sheet density in Fig. 2. The linear curve fits shown are only for the four lowest

Table 1
Summary for samples A–E of doping concentration defined in as grown well doping, equivalent sheet density, and average doping density for the whole active region, including threshold current density (J_{th}), maximum laser output current density (J_{max}), and maximum operating temperature (T_{max})

Sample	A	B	C	D	E
Doping of widest well ($\times 10^{15}\,cm^{-3}$)	2.80	4.24	6.40	10.00	25.00
Sheet density ($\times 10^{10}\,cm^{-2}$)	0.43	0.66	0.99	1.55	3.88
Average doping density ($\times 10^{15}\,cm^{-3}$)	0.79	1.20	1.82	2.84	7.10
J_{th} (kA/cm^2)	0.142	0.216	0.305	0.510	1.55
J_{max} (kA/cm^2)	0.292	0.379	0.566	0.832	2.01
T_{max} (K)	145	147	133	140	140

Download English Version:

https://daneshyari.com/en/article/1531339

Download Persian Version:

https://daneshyari.com/article/1531339

Daneshyari.com